Universidade Federal de Juiz de Fora
Programa de Pós-Graduação em Ecologia

José Reinaldo Paranaíba Vilela Alves Teixeira

HIGH SPATIAL VARIABILITY OF CARBON EMISSION AND GAS EXCHANGE COEFFICIENT IN THREE TROPICAL RESERVOIRS

Juiz de Fora
2017

Universidade Federal de Juiz de Fora
Programa de Pós-Graduação em Ecologia

José Reinaldo Paranaíba Vilela Alves Teixeira

HIGH SPATIAL VARIABILITY OF CARBON EMISSION AND GAS EXCHANGE COEFFICIENT IN THREE TROPICAL RESERVOIRS

Dissertação apresentada ao Programa de Pós-Graduação em Ecologia da Universidade Federal de Juiz de Fora, como parte dos requisitos necessários para obter o título de Mestre em Ecologia Aplicada ao Manejo e Conservação de Recursos Naturais.

Orientador: Prof. Dr. Nathan de Oliveira Barros

Co-orientadores: Prof. Dr. Fábio Roland e Prof. Dr. Sebastian Sobek

Juiz de Fora

2017

José Reinaldo Paranaíba Vilela Alves Teixeira

HIGH SPATIAL VARIABILITY OF CARBON EMISSION AND GAS EXCHANGE COEFFICIENT IN THREE TROPICAL RESERVOIRS

Dissertação apresentada ao Programa de Pós-Graduação em Ecologia da Universidade Federal de Juiz de Fora, como parte dos requisitos necessários para obter o título de Mestre em Ecologia Aplicada ao Manejo e Conservação de Recursos Naturais.

Examinadores

Dr. Felipe Siqueira Pacheco
Instituto de Pesquisas Espaciais

Dra. Raquel Fernandes Mendonça
Universidade Federal de Juiz de Fora

Prof. Dr. Fábio Roland (Co-orientador)
Universidade Federal de Juiz de Fora

Prof. Dr. Nathan de Oliveira Barros (Orientador)
Universidade Federal de Juiz de Fora

Ficha catalográfica elaborada através do programa de geração
automática da Biblioteca Universitária da UFJF,
com os dados fornecidos pelo(a) autor(a)

Paranaíba Vilela Alves Teixeira, José Reinaldo.
HIGH SPATIAL VARIABILITY OF CARBON EMISSION AND GAS EXCHANGE COEFFICIENT IN THREE TROPICAL RESERVOIRS / José Reinaldo Paranaíba Vilela Alves Teixeira. -- 2017.
64 f.

Orientador: Nathan Oliveira Barros
Coorientadores: Fábio Roland, Sebastian Sobek
Dissertação (mestrado acadêmico) - Universidade Federal de Juiz de Fora, Instituto de Ciências Biológicas. Programa de Pós Graduação em Ecologia, 2017.

1. Limnologia. 2. Reservatórios. 3. Gases de Efeito Estfa. 4. Emissão. 5. Variabilidade Espacial. I. Oliveira Barros, Nathan , orient. II. Roland, Fábio, coorient. III. Sobek, Sebastian , coorient. IV. Título.

The life is not important except in the impact it has on other lives.

Agradecimentos

Com muito orgulho, agradeço e dedico este trabalho aos meus pais Maria José e Israel, onde mesmo na ausência, sempre me ensinaram a ver a vida com alegria e amor. Agradeço também aos meus irmãos Adriana, Aislan e Iago pelo carinho e apoio em todas as dificuldades que enfrentei durante a minha vida.

Agradeço ao meu orientador Nathan Oliveira Barros, por sempre estar presente durante os últimos dois anos. Muito obrigado pela oportunidade de ser seu aluno, e por ter sido sempre paciente e compreensivo nos momentos de dificuldade. Quero também agradecer por ter me proporcionado a grande aventura e experiência de conhecer o outro lado do planeta, por ter sido sempre bem acolhido em sua casa junto à Raquel e Theo em Uppsala.

Agradeço ao meu co-orientador Fábio Roland pelos grandiosos conhecimentos compartilhados, pelas experiências vividas e por ter me acolhido na família LEA.

Aos amigos do Laboratório de Ecologia Aquática: André, Felipe, Gabrielle, Gladson, Guilherme, Ingrid, Iollanda, Ive, Maria, Nathália, Rafael, Simone e Polônia, pelos grandes momentos de conhecimento e diversão.

À Raquel Mendonça, por ter sido sempre presente neste trabalho. Muito obrigado pelos valiosos conhecimentos compartilhados, e em especial, pelos momentos vividos na Suécia.

Ao Carlos Henrique, pelos grandes momentos de aprendizado e descontração durante as coletas deste trabalho, e em especial pela amizade.

Aos barqueiros e amigos: Tiquinho (crustáceo), Sr. Tião, Sr. Neném, Alexandre, Cléber, Roseilson, Gonzaga e Charopinho pelos ensinamentos compartilhados nos reservatórios de Furnas e Curuá-Una.

Thanks to Sebastian Sobek, for receive me as a student and member of his project and for believe in my potential. Thank you for hosted me in Uppsala, and for provide one of the greatest experiences of my life.

Thanks to "Hydrocarb Team": Anastasija, Carolin, Charlotte, David, Gabriela, Jo, Ronnie, Stina, and especially Annika, for all experiences and knowledge shared during these two years.

Thanks to European Research Council for all support provided.

Obrigado Felipe Pacheco, por aceitar o convite para ser membro da banca e por revisar este trabalho.

Agradeço em especial à minha namorada Laura Chediak, por fazer parte deste trabalho e da minha vida, pelo amor, carinho, paciência e o enorme apoio emocional durante os últimos anos.

Agradeço a FAPEMIG pela bolsa de estudo oferecida durante os dois anos de trabalho. Obrigado PGECOL e LEA por viabilizarem este trabalho.

Abstract

Reservoirs are significant sources of carbon emission to the atmosphere. However the magnitude of this emission has huge uncertainties, partly related to the methods of sampling and partly related to the unconsidered spatial-temporal variability. Here we examined the spatial variability and its drivers of partial pressure, gas exchange coefficient and diffusive flux of CO_2 and CH_4 in three tropical reservoirs. We observed high spatial variability in CO_2 and CH_4 concentration and flux within the reservoirs. Our results suggest that all reservoirs were supersaturated in both gases, even considering that some areas were CO_2 sinks. A large spatial variability in k_{600} for CO_2 and CH_4, and consistently observed k_{600CH4} values higher than k_{600CO2} were also observed in all reservoirs. We could explain the high spatial variability of CO_2 and CH_4 by a combination of parameters such as dissolved oxygen, pH, chlorophyll, wind speed and bathymetry. Finally, we suggest a minimum sampling effort required to representatively cover a study site. Our results illustrate the first specially-resolved analysis of CH_4 emissions in reservoirs, and we suggest that in large systems (area $\geq$ 1,000 km²) and small systems (area $\leq$ 100 km²), 600 and 200 measurements sites, respectively, are need for a representative dry period carbon flux estimates.

Summary

Figure List:

Table List:

1. Introduction

Reservoirs are sites of intense carbon processing, with substantial influence on the global carbon (C) budget (Louis et al. 2000; Barros et al. 2011; Deemer et al. 2016). Collectively, reservoirs emit to the atmosphere 51 Tg of C yr^{-1}, of which 36.8 Tg of C y^{-1} is emitted as carbon dioxide (CO_2) and 13.3 Tg of C yr^{-1} as methane (CH_4) (Deemer et al. 2016). During the first years after the construction of a dam, C emission from reservoirs result mainly from the decomposition of flooded vegetation and soil organic matter (OM). As the reservoirs age, continued OM inputs from inflowing rivers, production of aquatic plants (phytoplankton and macrophytes), and regrowth of land plants along shores during draw-down periods become the main sources of organic carbon (OC), which then fuels C emission from reservoirs. As consequence of the variable OC sources, which are unevenly distributed along reservoirs, C emissions are expected to show high spatial heterogeneity (e.g. Roaland et al. 2010, Teodoru et al. 2011, Pacheco et al. 2015).

These fluxes vary greatly in both space and time, and the spatial-temporal variability is not well represented in the global-scale estimates of reservoir emissions, resulting in large uncertainty (Bastviken et al. 2011; Raymond et al. 2013). Carbon emission from reservoirs has historically been linked to reservoir age, latitude, dissolved OM availability, and water depth (Barros et al. 2011). Recently, reservoir productivity, which is related to nutrient loading and eutrophication, was demonstrated to enhance emissions, especially in CH_4 (Almeida et al. 2016; Deemer et al. 2016). Although CH_4 emissions from reservoirs are generally lower in terms of carbon units when compared to CO_2 emissions, the up to 34 times higher global warming potential on a 100 years basis makes CH_4 the gas of primary concern with respect to reservoir emissions (Myhre et al. 2013).

Diffusion is the dominant pathway for CO_2 emission from both lakes and reservoirs and is also important CH_4 emission pathway, even though ebullition has been shown to often be the dominant pathway for CH_4 emission (Bastviken et al. 2004; Deemer et al. 2016). In fact, a large number of published studies present diffusive flux estimates only (Deemer et al. 2016). This is probably attributable to the relative ease of calculating diffusive emission. The diffusion of CO_2 and CH_4 from reservoirs results from the concentration gradient between the surface water and the atmosphere (Cole et al. 1994), and the rate of diffusion is generally controlled by the saturation level in the surface water and the gas exchange velocity, which largely depends on water-side turbulence (Cole and Caraco 1998; Algesten et al. 2005; Sobek, Tranvik, and Cole 2005; Abril, Richard, and Guérin 2006). Hence, a few gas concentration measurements and a single value for gas transfer velocity scaled from wind speed (e.g., Cole and Caraco) are sufficient to calculate diffusive emission for an entire reservoir. However, the simplicity of this method is deceptive. Often, fewer than 5 or 10 sites per reservoir are sampled for concentration measurements (Deemer et al. 2016), and often near the dam because of easy access. This is problematic because C dynamics and thus CO_2 and CH_4 concentrations in freshwater are results of complex interactions between local hydrological and biogeochemical processes (Borges et al. 2015). Thus, different regions of the reservoir show different C dynamics in the water column (Pacheco et al. 2015), owing to the type of the flooded biomass and sediment, organic and inorganic material inputs from rivers, primary production, bacterial respiration and dam operation regime (Roland et al. 2010). For example, in river inflow areas the OC is imported from the catchment, leading to high sediment deposition and CH_4 production (DelSontro et al. 2011; Sobek et al. 2012; Maeck, Hofmann, and Lorke 2014).

The scaling of the gas exchange velocity from wind speed in itself is highly uncertain (Cole and Caraco 1998), and wind speed measurements are often done at few

sites (if not only one site or by a meteorological station nearby) with limited spatial resolution. Wind patterns are complex, however. Whereas elevated water-side turbulence and gas exchange velocity can be expected at river inflow areas or in open, wind-exposed areas, low water turbulence and gas exchange velocity are expected in narrow, wind-protected bays. Such variabilities are unaccounted for at present, and the resulting diffusion estimates are consequently uncertain. Alternatively, floating chambers (FC) are frequently used to measure diffusive emission, as well as the sum of diffusive and ebullitive emission. Even though FC represent a direct measurement of flux, they are only capable of covering a small window in space and time. In order to account for the complex dynamics of the parameters that modify the rate of greenhouse gas (GHG) emission for large impoundments, a large representative area needs to be covered by sampling (Roland et al. 2010; Teodoru, Prairie, and Del Giorgio 2011).

Particularly tropical reservoirs have been reported to be strong GHG sources (Barros et al. 2011; Fearnside and Pueyo 2012), but even though such a pattern was not evident in the most recent global compilation of reservoir emission (Deemer et al. 2016), data from tropical reservoirs are relatively scarce. Given the large number of existing reservoirs in the tropics and the projected increase in hydropower production in tropical countries (MME 2013; Hu and Cheng 2013), more studies of greenhouse gas emission from reservoirs in tropical regions are needed.

1.1 Hypothesis and Goals

Here, we test the hypothesis that the diffusive emission of CO_2 and CH_4 from tropical reservoirs is characterized by strong spatial variability, and that emissions are incorrectly represented if measurements are only made close to the dam. We studied three tropical reservoirs located in different biomes of Brazil (Amazon, Savannah and Atlantic Forest).

We used spatially resolved concentration measurements with an on-line equilibration system in combination with spatially resolved measurements of the gas exchange velocity with floating chambers. We compared our estimates with calculations using one gas exchange velocity based on average wind speed, and concentration measurements at only a single site at the dam of each reservoir. Furthermore, we give recommendations for the minimum spatial coverage needed to adequately represent diffusive fluxes of CO_2 and CH_4 from each reservoir.

2. Experimental section

2.1 Study sites

We studied three tropical reservoirs located in different biomes in Brazil: Chapéu D'Úvas (CDU), Curuá-Una (CUN) and Furnas (FNS) (Table 1). CDU is a 12 km^2 oligotrophic drinking water reservoir located in the Atlantic Forest biome. CUN is a 72 km^2 oligotrophic hydroelectric reservoir located in the Amazon. FNS is a 1,342 km^2 hydroelectric reservoir located in the Cerrado (Savannah-type) biome, with two river inflows that are of different trophic state (northern arm: mesotrophic; southern arm: eutrophic) (Figure 1). CDU and FNS reservoirs are characterized by a rainy period in summer and a dry period in winter and CUN is described by rainy throughout the year (IBGE 2012).

Table 1: Location and features of the reservoirs

	CDU	CUN	FNS
Coordinates	S 21	3S'2 W 43 35'	56'20W 54 18'
Biome	Atlantic Forest	Amazonia	Cerrado (Savannah)
Year of operation	1994	1977	1963
Reservoir use	Water supply	Hydroelectricity	Hydroelectricity
Area (km^2)	12	72	1,342
Volume (km^3)	0.146	0.472	20.7
Watershed area (km^2)		15,300	51,773
Maximum depth (m)	41	36	89
Mean depth (m)	19	6	15
Residence time (years)		29	1,38
Elevation (m)	682	68	755
Mean total phosphorus (µg L^{-1})	12	19	39
Mean total nitrogen (µg L^{-1})	452	661	1,204
Annual mean air temperature (C)	18	28	20
Annual precipitation (mm)	1,600	2,200	1,126

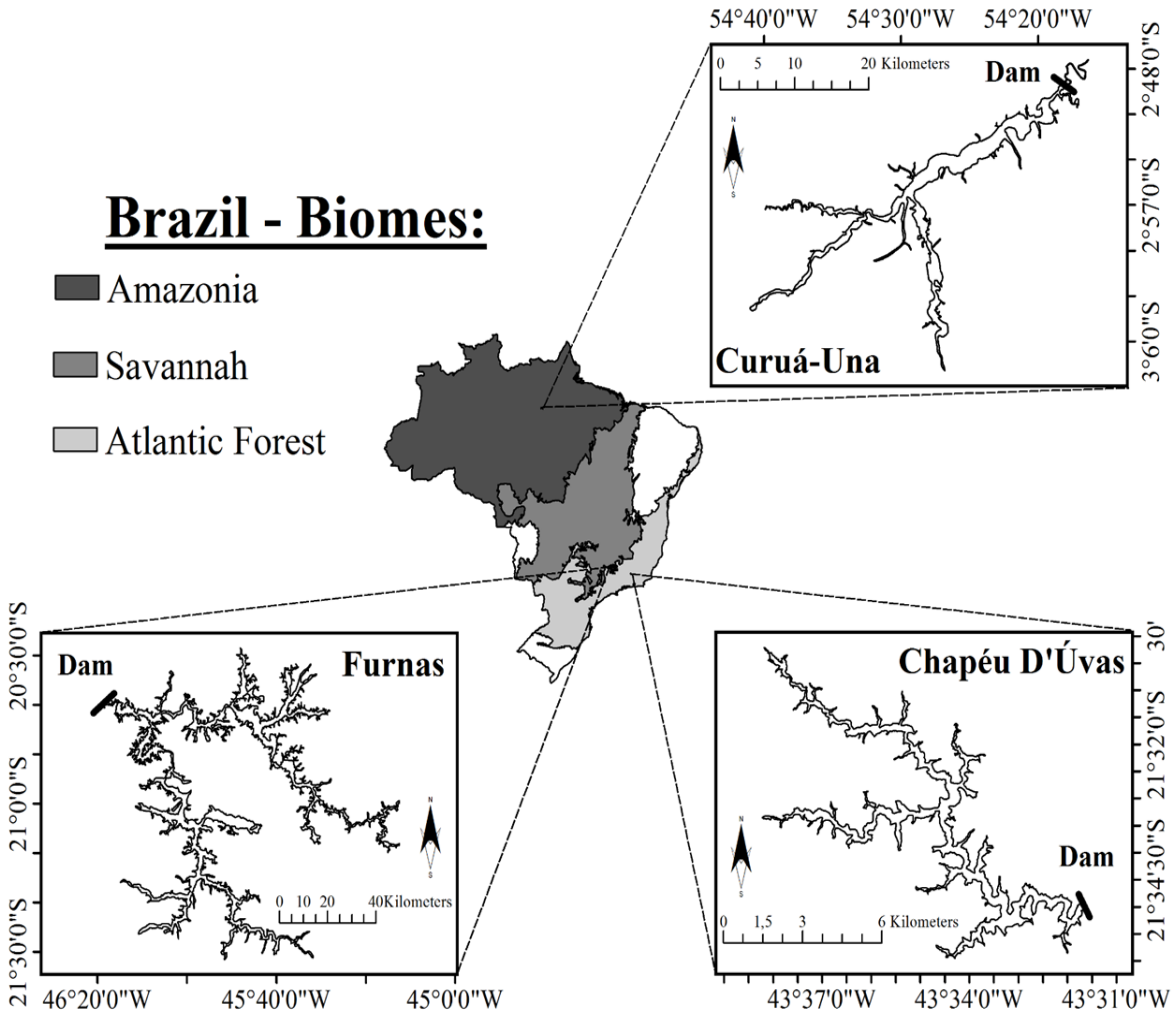

Figure 1: Location of the studied reservoirs, in three different biomes: Amazonian biome, Savannah biome and Atlantic Forest biome.

2.2 Measurements

One field campaign was conducted in each reservoir (CDU: September 2015; CUN: March 2016: FNS: June/July 2015) during the low water season with a rising water level (Figure 2).

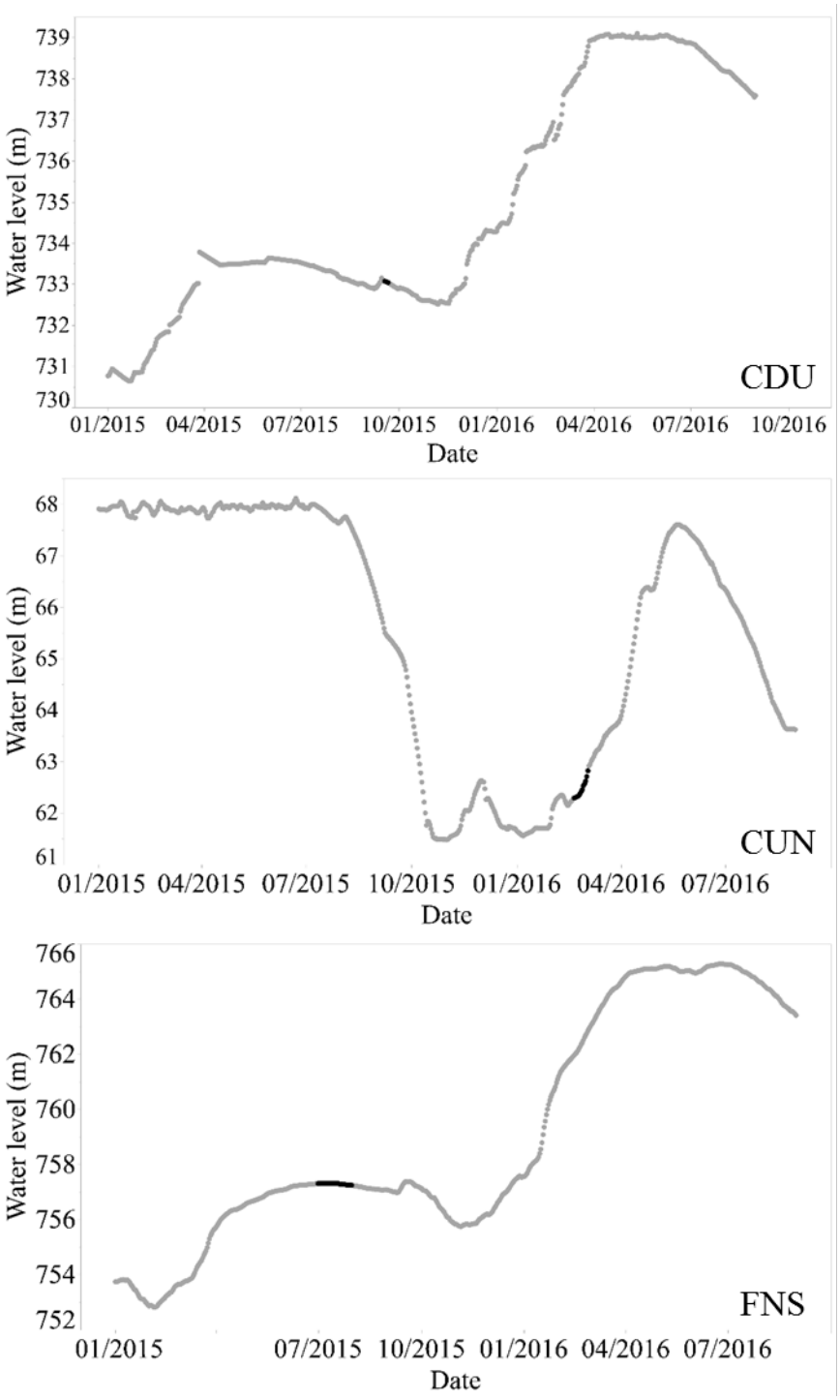

Figure 2: Water level fluctuation from CDU, CUN and FNS. The black circles indicate fieldwork periods.

2.3 Equilibrator-based CO_2 and CH_4 concentrations (pCO_2 and pCH_4)

We used an on-line equilibration system connected to an ultra-portable greenhouse gas analyzer (UGGA, Los Gatos Research) to perform continuous measurements of CO_2 and CH_4 partial pressure (pCO_2 and pCH_4) in water as the boat moved through each of the reservoirs (zigzag-pattern surveys, Figure 3).

Water from ~0.5 m depth was pumped continuously (3 L min^{-1}) through a pre-filter and a cartridge filter (10 µm pore size, Eaton Lofwind), and further to a membrane-based equilibrator (Permselect module PDMS-XA 1.0, Medarray Inc), composed of an array of silicone hollow fibers with a total exchange area of 1 m^2. The water flows outside the hollow fibers, while the gas flows inside the hollow fibers towards the UGGA (similar setup described by Gonzalez-Valencia et al. 2014). The gas flew in an open gas loop, i.e. gas was not circulated back to the equilibrator after passing the UGGA. The UGGA output data were logged with 1 Hz frequency using the software Coolterm 1.4.7, and geographic coordinates were recorded concomitantly, using a handheld GPS device (Garmin, eTrex 30x).

The response time of the on-line equilibration system was 3 minutes for CO_2 and 5 minutes for CH_4, with an equilibration efficiency of 84% (SD: ± 14) for CO_2 and 87% for CH_4 (SD: ± 12). We determined the equilibration efficiency by comparing equilibrator-derived CO_2 and CH_4 concentrations with concentrations derived from manual samples (see below).

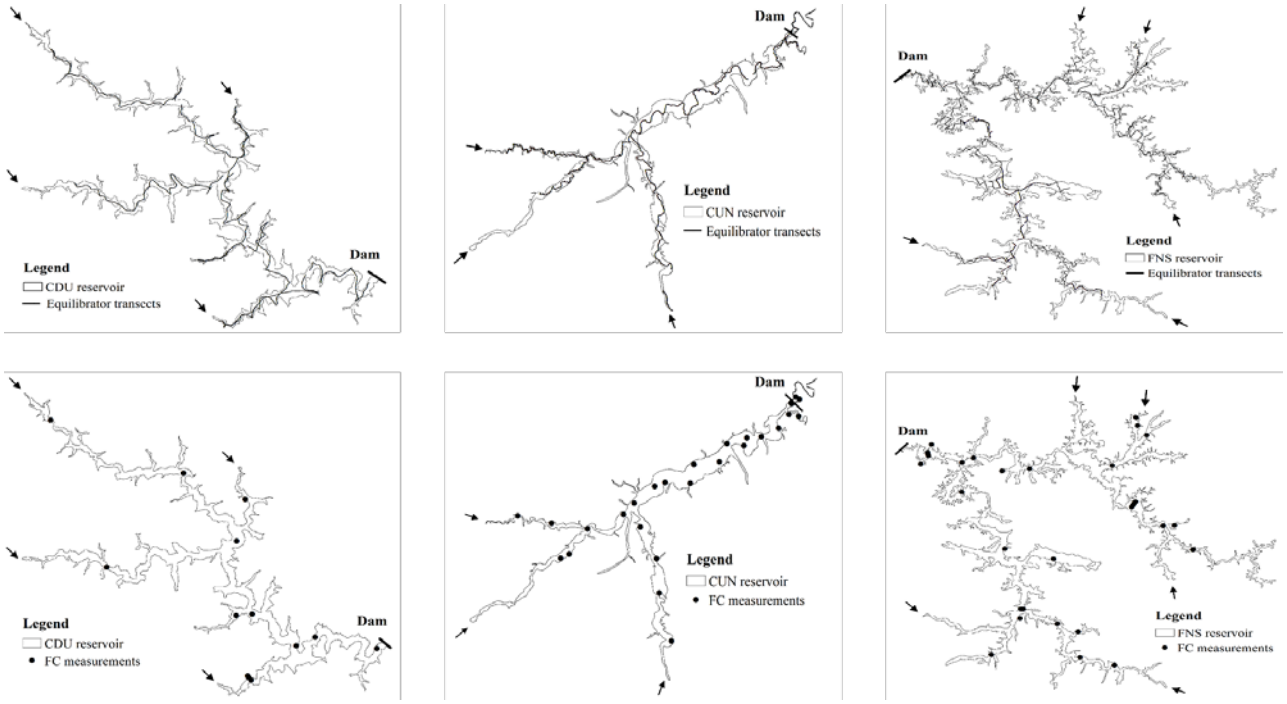

Figure 3: Sampling strategy performed in CDU, CUN and FNS. The solid black line represents the equilibrator transects and the black circles represents floating chambers and discrete samples measurements. The black arrows represents the river entrances in these systems.

2.4 Discrete samples of pCO_2 and pCH_4

In addition to equilibrator-based measurements, we measured pCO_2 and pCH_4 manually, applying the headspace equilibration technique (Cole and Caraco 1998), at approximately every kilometer along the length of each reservoir (n = 39 in CDU, n = 90 in CUN and n = 99 in FNS). At each measurement site, we filled a 60 mL syringe with 30 mL surface water and 10 mL atmospheric air. The syringe was then vigorously shaken for 60 seconds to allow the gas and water phase to equilibrate and then the 10 mL headspace was transferred to a second syringe and injected in the UGGA. For this purpose, the UGGA was equipped with a custom-made inlet port connected to a carrier gas flow consisting of CO_2-free air (ambient air passing through a soda lime cartridge) and driven by its internal pump. The resulting baselines were zero for CO_2, and atmospheric concentration for CH_4 (~1.8 ± 0.1 ppm). The peaks recorded by the UGGA were integrated and compared to a calibration curve to determine the pCO_2 and pCH_4. We used the solubility coefficient of

Weiss 1974 to compute the water surface concentrations of CO_2, and the surface concentrations of CH_4 were calculated according to the solubility coefficient from Yamamoto et al. 1976 (Yamamoto, Alcauskas, and Crozier 1976). Detection limits for manual injection into the UGGA were 1.5 x 10^{-7} mol L^{-1} and 2.76 x 10^{-10} mol L^{-1} for dissolved CO_2 and CH_4 concentration, respectively.

2.5 Calculation of the gas exchange coefficient (k)

We performed FC measurements, which give direct estimates of CO_2 and CH_4 flux across the air-water interface and allow for the determination of the gas exchange coefficient *k* (Cole et al. 2010). FCs were deployed every 1 km distances, including sites of open water, flooded forests, land-water boundaries and river entrances (n = 39 in CDU, n = 90 in CUN and n = 99 in FNS). The transparent acrylic FCs had walls extending 4-5 cm into the water column (17 L total volume, 0.07 m^2 surface area, and circular design). The FC was left drifting during measurement to avoid creation of artificial turbulence. It was connected to the UGGA with a closed gas loop to quantify changes in CO_2 and CH_4 concentration inside the chamber over about 5 minutes. Real-time display of concentrations inside the chamber allowed keeping each chamber deployment as short as possible. We deployed our FC three times at each site. Chamber deployments were discarded if a linear regression between concentration increase and time rendered $r^2 < 0.9$, indicating non-linear behavior that is probably related to gas bubbles enriched in CH_4 and CO_2 entering the chamber (Guérin et al. 2007).

The diffusive gas flux depends on two main factors: the concentration gradient over the air-water interface and the gas exchange coefficient (*piston velocity*) for a given gas at a given temperature. This gradient is expressed as the difference between the actual concentration of gas in the water and the concentration that water should have if it was in

equilibrium with the atmosphere. According to Cole et al. 2010, *k* can be estimated applying FCs. Thus, the flux across the air-water interface can be calculated following the equation proposed by Cole and Caraco 1998:

$$F_{g,T} = k(C_w - C_{eq}) \quad (1)$$

where $F_{g,T}$ is the flux at the air-water interface for a given gas (*g*) at a given temperature (*T*) (mmol m^{-2} day^{-1}), *k* is the gas exchange coefficient for the given gas (m day^{-1}), C_w is the concentration of the given gas in water (mmol m^{-3}); C_{eq} is the theoretical concentration of the given gas in water if the water phase was in equilibrium with the atmosphere (mmol m^{-3}).

Gas exchange velocities were derived from concomitant measurements of gas flux (by FC measurements) and of the measured partial pressure for both pCO_2 and pCH_4. Thus, k_{FC} can be calculated as follows:

$$k_{FC} = (C_w - C_{eq})/F_{g,T} \quad (2)$$

To compare *k* for CO_2 and CH_4, piston velocity was normalized to a Schmidt number of 600 for both CO_2 and CH_4 at 20 °C according to Jähne et al. 1987:

$$k_{600} = k_{FCg,T}(600/Sc_{g,T})^{-n} \quad (3)$$

where $Sc_{g,T}$ is the Schmidt number for a given gas at a given temperature (Wanninkhof 1992). We assumed $n = 2/3$ for wind speed at 10 m < 3.7 m s^{-1}, and $n = 1/2$ for wind speed at 10 m > 3.7 m s^{-1} (Guérin et al. 2007; Prairie and del Giorgio 2013; McGinnis et al.

2015). k_{600} was calculated for both gases, i.e. from CO_2 flux and CO_2 concentrations (termed k_{600CO_2}) and from CH_4 flux and CH_4 concentrations (termed k_{600CH_4}).

2.6 Bathymetry analysis

Bathymetric surveys were performed in each reservoir using a 10 kHz portable high resolution sub-bottom seismic profiler (Strat-aBox, SyQuest). Shore-to-shore transects were made at 2 km h^{-1} along the entire reservoir and the seismic output data logging were georeferenced, highlighting the need to generate a high-resolution map.

2.7 Environmental and limnological variables

We measured air temperature and wind speed at 2 m above water surface with a portable anemometer (Skymaster – Speedtech SM-28, accuracy: 3%) every 1 kilometer distance, as described above. Wind speed measurements were normalized to wind speed at 10 m above water level according to Smith 1985 equation. Surface water temperature, conductivity, turbidity, pH, chlorophyll *a*, and dissolved oxygen concentrations were determined using a multi-parameter probe (YSI 6600 V2). It is important to note that optical sensors for chlorophyll *a* and dissolved oxygen were used during the measurements.

Surface water samples were collected using polypropylene bottles (300 mL) every kilometer traveled. In the laboratory, the samples were analyzed for total phosphorus (TP), total nitrogen (TN) and total organic carbon (TOC). TP and TN samples were analyzed in spectrophotometer (Beckman Coulter, DU - 640) following potassium persulfate digestion (TP and alkaline persulfate digestion (TN)). TOC samples were analyzed by high temperature combustion on a total carbon analyzer (Shimadzu, TOC-L CPH/ASI-L).

2.8 Data analysis and statistical procedures

Data interpolation to create maps of CO_2 and CH_4 partial pressure, k_{FC} and bathymetry was performed using the Inverse Distance Weighted algorithm (IDW, cell size approximately 37 x 37 m) (Xiong et al. 2012), using the software ArcGIS (v10.2, ESRI). The interpolation accuracy from IDW analyzes were compared with Kriging analyzes through each root mean square for each parameter interpolated (Figure 4).

Maps of diffusive fluxes of CO_2 and CH_4 were created by combining each grid cell of partial pressure maps with the corresponding grid cell of k_{FC} maps, following equation (1). Finally, we extracted the cell values from all maps (partial pressure, *k*, diffusive fluxes and bathymetry) in order to obtain data from all reservoirs with the same spatial resolution (~37 m), which were then used in the analysis.

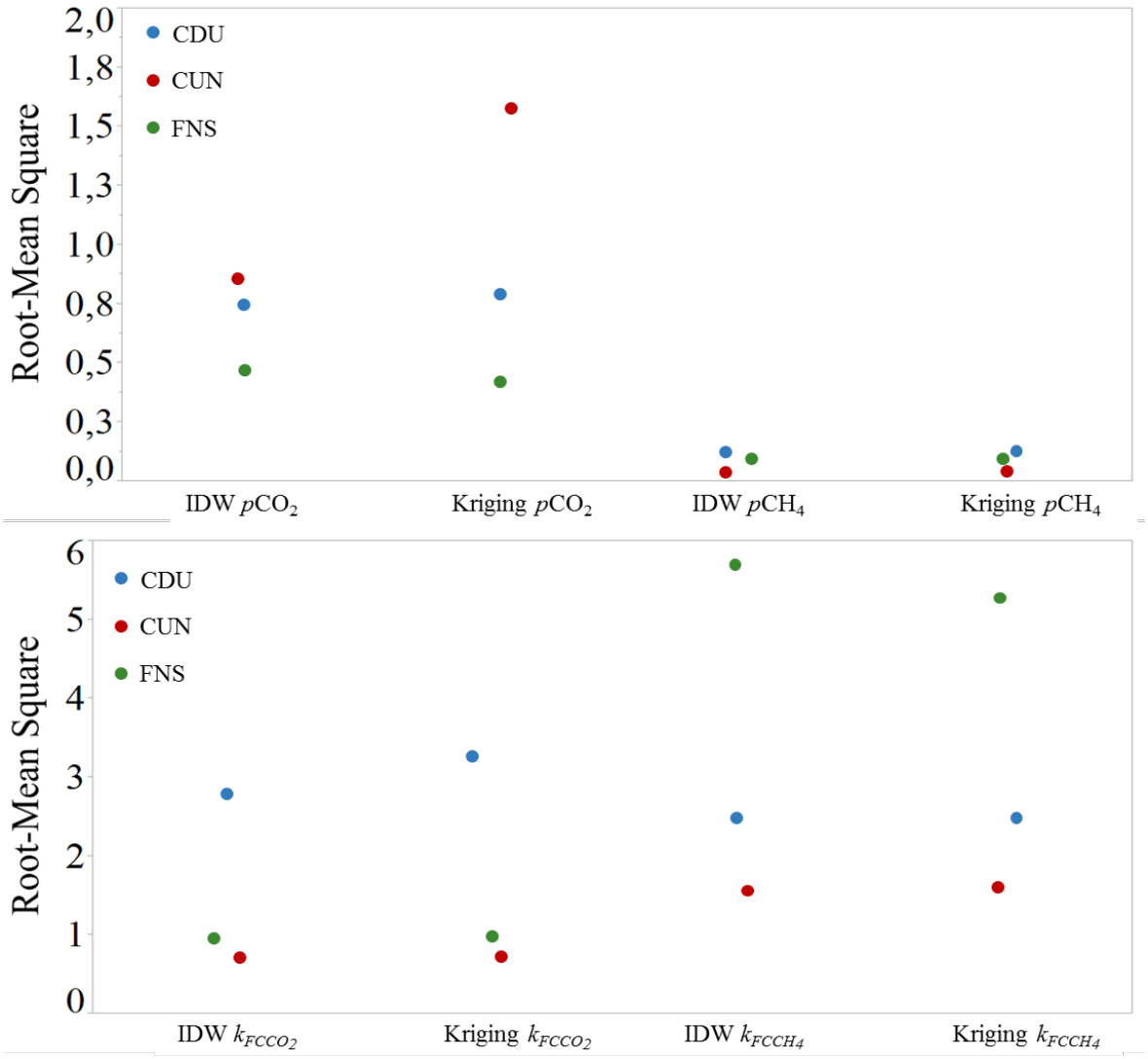

Figure 4: Interpolation accuracy of Inverse Distance Weighted (IDW) and Kriging analyzes from pCO_2, pCH_4, k_{FCCO2} and k_{FCCH4} in CDU, CUN and FNS.

The potential drivers of variability in CO_2 and CH_4 concentrations within reservoirs were investigated using partial least squares regression (PLS) performed for each gas and each reservoir separately (Höskuldsson 1988). The variables included in the PLS were measurement date and time, latitude and longitude, water temperature, pH, conductivity, chlorophyll a, turbidity, dissolved oxygen concentration and dissolved oxygen saturation. Measurement date and time were included as means of testing the effect of changes in weather during the period of sampling (the results show the spatial variability, but also include some temporal variability).

In order to estimate the minimum number of sampling required to perform a representative spatial coverage of all reservoirs, we used a binary model of data simulation, based on hypothetical scenarios created to determine the effect of different sampling effort with different significant level (Wik et al. 2016). Diffusive flux measurements of CO_2 and CH_4 from all reservoirs (*n*CDU = 21827; *n*CUN = 106373; *n*FNS = 87274) were added in several compartments, where each compartment represents a different scenario based on an increasing number of diffusive flux measurements. We considered the level of confidence corresponding to 90% of average fluxes within ± 20% of spatial average in each reservoir, as values substantially representative of total spatial variability. Finally, we selected different regions of the size of CDU (smallest reservoir) in CUN and FNS in order to evaluate the reservoir size dependence in spatial variability of diffusive fluxes of CO_2 and CH_4 in different systems.

Statistical analyses were performed using the software JMP (Version 12.1.0). For all statistical tests, we assumed $p < 0.05$ as the threshold level for acceptance.

3. Results

3.1 Variability of pCO_2 and pCH_4

The pCO_2 varied from 300 to 773 µatm in CDU (mean ± SD: 439 ± 63), from 387 to 1478 µatm in CUN (664 ± 221), and from 7 to 3090 µatm in FNS (400 ± 299) (Figure 5). The pCH_4 varied from 2 to 65 µatm in CDU (11 ± 9), from 1.8 to 50 µatm in CUN (9 ± 5), and from 1.8 to 217 µatm in FNS (30 ± 20) (Figure 5). Expressed as the coefficient of variation, the range of variability within the reservoirs varied between 0.1 (CDU) and 0.8 (FNS) for pCO_2, and between 0.5 (CUN) and 0.8 (CDU) for pCH_4 (Table 2). In general, there was a tendency of higher pCO_2 and pCH_4 in river inflows areas and decreasing values towards the dam. An exception is the pCO_2 in FNS, which increased towards to the dam (Figure 6). The overall mean pCO_2 and pCH_4 in all three reservoirs were 4.5 times and 9 times higher than atmospheric equilibrium, respectively.

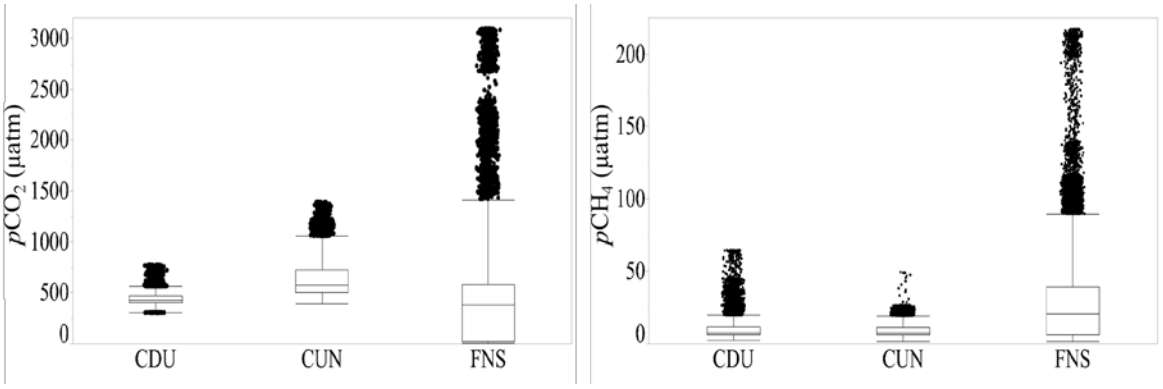

Figure 5: Box plot of pCO_2 and pCH_4 (µatm) from equilibrator measurements of CDU, CUN and FNS reservoirs. Atmospheric equilibrium of pCO_2 and pCH_4 were 399 µatm and 1.8 µatm, respectively.

Table 2: Average, standard deviation and median of pCO_2 and pCH_4 (µatm), coefficient of variation of pCO_2 and pCH_4, TOC – main tributary and before dam (mg C L^{-1}), Wind Speed at 10 m (m s^{-1}), k600 from CO_2 and CH_4 (m day^{-1}) and k_{600CH4}/k_{600CO2} ratio.

	Reservoirs		
	CDU	**CUN**	**FNS**
***p* CO_2 (µatm)**	439 ± 63	664 ± 221	400 ± 299
median	423	587	380
***p* CH_4 (µatm)**	11 ± 9	9 ± 5	30 ± 20
median	7	7	20
Coefficient of variation of *p* CO_2	0.1	0.3	0.8
Coefficient of variation of *p* CH_4	0.8	0.5	0.7
TOC - main tributary (mg C L^{-1})[a]	3.2 ± 0.5	4.3 ± 0.8	3.5 ± 0.4
median	3	4	2.8
TOC - reservoir before the dam (mg C L^{-1})[a]	1.1 ± 0.3	2.1 ± 1	1.4 ± 0.2
median	0.8	1.8	1
Wind speed at 10-m (m s^{-1})	2.7 ± 2.4	4.4 ± 2	1.3 ± 2.1
median	2.4	3.8	1.4
$k_{600\ CO2}$ value (m day^{-1})	0.9 ± 0.6	0.5 ± 0.6	1.1 ± 1.2
median	0.5	0.4	0.6
$k_{600\ CH4}$ value (m day^{-1})	2.8 ± 1.6	1.4 ± 1	3 ± 3.3
median	3.4	1.3	1.5
k_{600CH4}/k_{600CO2} ratio	3.1	2.8	2.7

[a] *This study*

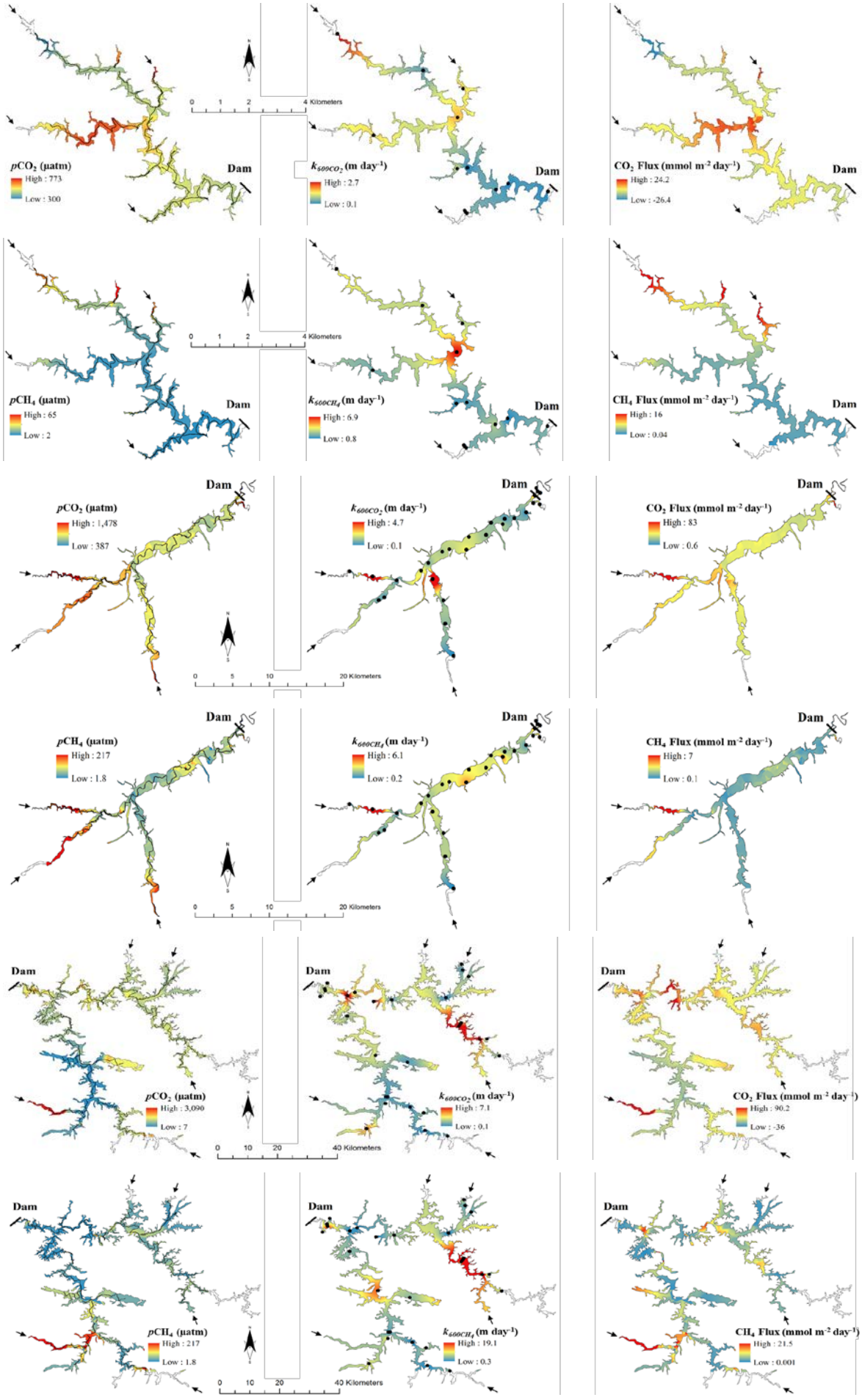

Figure 6: pCO_2 and pCH_4 (µatm), k_{600CO2} and k_{600CH4} (m day^{-1}), and diffusive flux of CO_2 and CH_4 (mmol m^{-2} day^{-1}) in a spatial scale expressed by a color gradient obtained from an interpolation of measured data using the Inverse Distance Weighted (IDW) in CDU, CUN and FNS reservoir.

3.2 Gas exchange coefficient (k_{600})

k_{600} calculated from CO_2 varied from 0.1 to 2.7 m day^{-1} (0.9 ± 0.6) in CDU, from 0.1 to 4.7 m day^{-1} (0.5 ± 0.6) in CUN and from 0.1 to 7.9 m day^{-1} (1.1 ± 1.2) in FNS. If calculated from CH_4 measurements, k_{600} varied from 0.8 to 6.9 m day^{-1} in CDU (2.8 ± 1.6), from 0.2 to 6.1 m day^{-1} in CUN (1.4 ± 1) and from 0.3 to 19.1 m day^{-1} in FNS (3 ± 3.3). While there were no distinct patterns in space, we could sometimes observe higher k_{600} in large open waters and river inflow areas (e.g. in CDU – Figure 6).

3.3 Diffusive flux of CO_2 and CH_4

The diffusive flux of CO_2 varied from -26.4 to 24.2 mmol m^{-2} day^{-1} (4.8 ± 6) in CDU, from 0.6 to 82.8 mmol m^{-2} day^{-1} (7.7 ± 9.5) in CUN and from -36 to 90.2 mmol m^{-2} day^{-1} (7.1 ± 15.8) in FNS. For CH_4, the diffusive flux ranged from 0.04 to 16 mmol m^{-2} day^{-1} (1.6 ± 1.7) in CDU, from 0.09 to 6.9 mmol m^{-2} day^{-1} (0.6 ± 0.8) in CUN and from 0.001 to 21.5 mmol m^{-2} day^{-1} (2.5 ± 2.5) in FNS. The CO_2 and CH_4 diffusive fluxes observed in all reservoirs show large variability, resulting from the variabilities in concentrations and gas exchange velocities (Figure 6).

3.4 Persistence of higher k_{600CH4} than k_{600CO2}

The k_{600CH4} and k_{600CO2} values were significantly correlated with each other (r^2 = 0.519 $p < 0.0001$) but deviated strongly from the 1:1 line. The k_{600} values derived from CH_4 were higher than the k_{600} derived from CO_2 in more than 98 % of the measurements (Figure 7). The ratio k_{600CH4} / k_{600CO2} was similar in each reservoir, with averages ranging from 2.7 to 3.1 (Table 2).

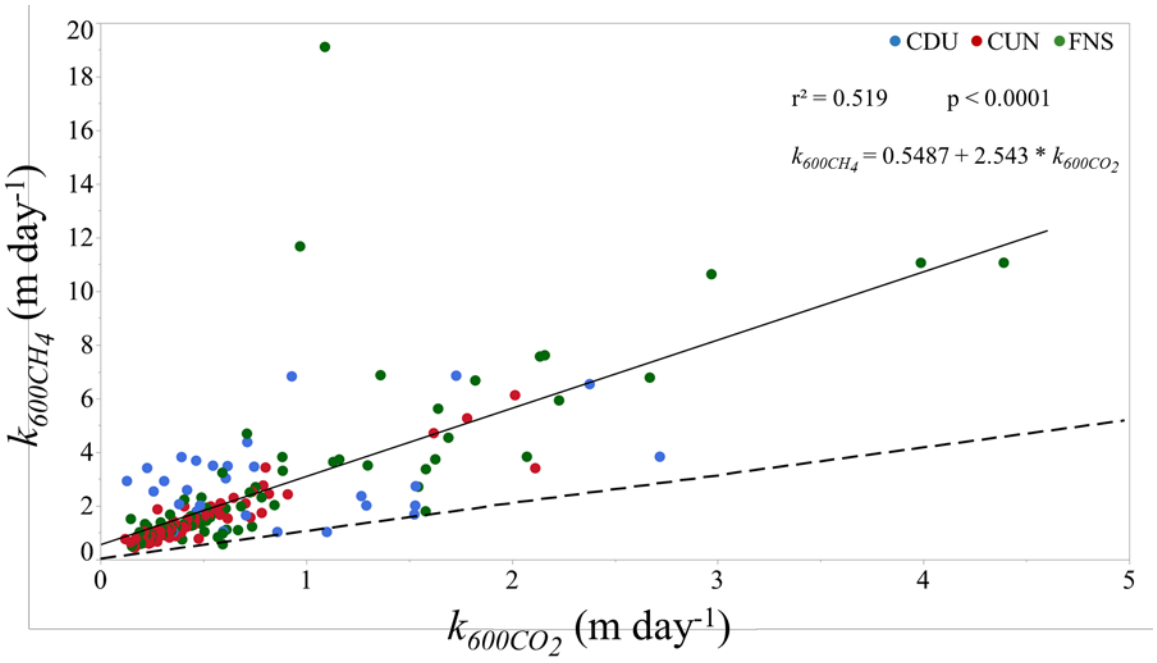

Figure 7: Relationship between the gas exchange velocity k_{600CH4} (y axis) and k_{600CO2} (x axis) for CDU, CUN and FNS. The dashed line represent the equality line.

3.5 Drivers of within-reservoir variability

The variability in pCO_2 could be explained well (r^2Y of 0.64-0.81) in each reservoir, and for all three reservoirs, we detected strong negative relationships with dissolved O_2 (Table 3). Negative relationships with pH and with date or time were apparent in some of the reservoirs (Table 3). The variability in pCH_4 could also be well explained in each reservoir (r^2Y of 0.41-0.79), and the geographic coordinates were strongly connected to the variability in pCH_4 in all reservoirs. If removing the geographic coordinates from the PLS model, model performance dropped drastically to r^2Y of 0.12-0.55. In addition, pH as well as date and time were important for explaining variability in pCH_4, albeit not consistently in all reservoirs. The Q^2 values of all PLS models were similar to the r^2Y values, indicating high predictive power.

Table 3: Parameters of PLS models explaining the variability in log10-transformed pCO_2 and pCH_4 in the studied reservoirs. Variable importance in projection (VIP) describes how much a variable contributes to explaining the Y variable.

Reservoir	**CDU**		**CUN**		**FNS**		**CDU**		**CUN**		**FNS**	
Model	$\log p\,CO_2$		$\log p\,CO_2$		$\log p\,CO_2$		$\log p\,CH_4$		$\log p\,CH_4$		$\log p\,CH_4$	
Components	9		3		5		3		4		3	
r^2Y	0,64		0,81		0,75		0,79		0,65		0,41	
Q^2	0,64		0,81		0,75		0,79		0,65		0,41	
Parameter	VIP	Coefficients	VIP	Coefficients	VIP	Coefficients	VIP	Coefficients	VIP	Coefficients	VIP	Coefficients
Date	1,12	0,05	1,24	0,03	0,80	-0,12	1,79	0,08	0,98	-0,03	0,86	0,01
Time	1,52	0,07	0,09	0,00	0,93	-0,18	0,61	-0,02	1,00	-0,04	0,66	-0,05
GPS(S)	0,61	-0,03	0,73	-0,01	0,72	-0,29	1,89	0,09	1,06	-0,05	1,67	-0,18
GPS(W)	0,66	0,04	1,20	0,02	0,51	-0,05	1,58	-0,08	1,02	-0,02	0,74	-0,001
Water temperature	1,00	0,01	0,85	0,00	0,82	0,09	0,43	0,02	1,02	-0,03	0,62	-0,04
pH	0,50	-0,01	1,29	-0,02	1,56	-0,39	0,48	0,04	1,03	-0,02	1,28	0,13
log CH_4	0,71	0,02	1,35	0,05	0,85	-0,16	0,67	0,004	1,60	0,15	1,41	-0,18
Conductivity	1,01	-0,01	0,67	0,00	0,72	0,03	0,40	-0,02	0,81	-0,01	0,41	-0,02
log Chl a	0,69	-0,01	0,57	0,03	0,64	0,04	0,49	-0,01	0,36	0,03	0,62	0,04
log Tubidity	0,85	0,00	0,11	-0,01	0,43	0,01	0,50	0,01	0,05	-0,005	1,16	0,02
[O_2]	1,62	-0,02	1,31	-0,03	1,53	-0,07	0,58	0,02	1,07	0,04	0,88	-0,05
%O_2 sat	0,99	-0,01	1,29	-0,02	1,55	-0,07	0,64	0,04	1,08	0,03	0,85	-0,06
Intercept		2,63		2,79		2,09		0,94		0,91		1,31

We additionally looked for statistical drivers of within-reservoir variability in k_{600}, but the resulting statistical models were weak (data not shown). In most cases, PLS models did either not converge or permutation tests showed that random data generated models of similar explanatory power. While there were positive relationships between k_{600} and wind speed, the great spread in these relationships makes wind speed a poor predictor of k_{600} (Figure 8).

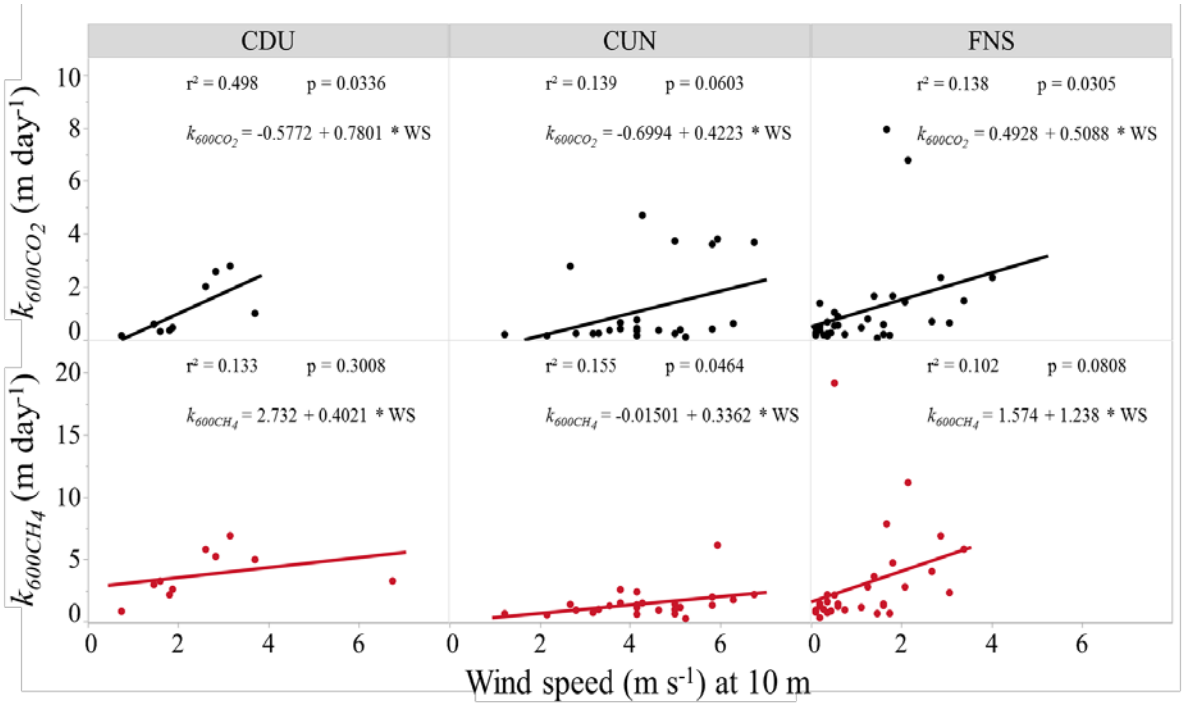

Figure 8: Relationship between wind speed and k_{600CO2} and k_{600CH4} measured by floating chambers. Every point represents the mean of 3 chamber deployments at each measurement location.

3.6 Sampling effort

Through the simulation of several hypothetical scenarios with diffusive flux of CO_2 and CH_4, we found that in CDU, at least 90 CO_2 flux data per sampling period are required to achieve 90% confidence of fluxes within ± 20% accuracy achieved with the complete database. For CUN, 180 CO_2 flux data are required to achieve a representative value, and 900 CO_2 flux data points are required for FNS (Figure 9). When calculated for diffusive

fluxes of CH_4, 100 flux data are required for CDU, 190 flux data are required for CUN and 190 flux data are required for FNS to achieve high reliability over the total spatial distribution obtained in each reservoir (Figure 9). We also found that different sections in CUN and FNS with the same size of CDU required different numbers of minimum sampling efforts to reach the 90% confidence of fluxes within ± 20% accuracy (Figure 10).

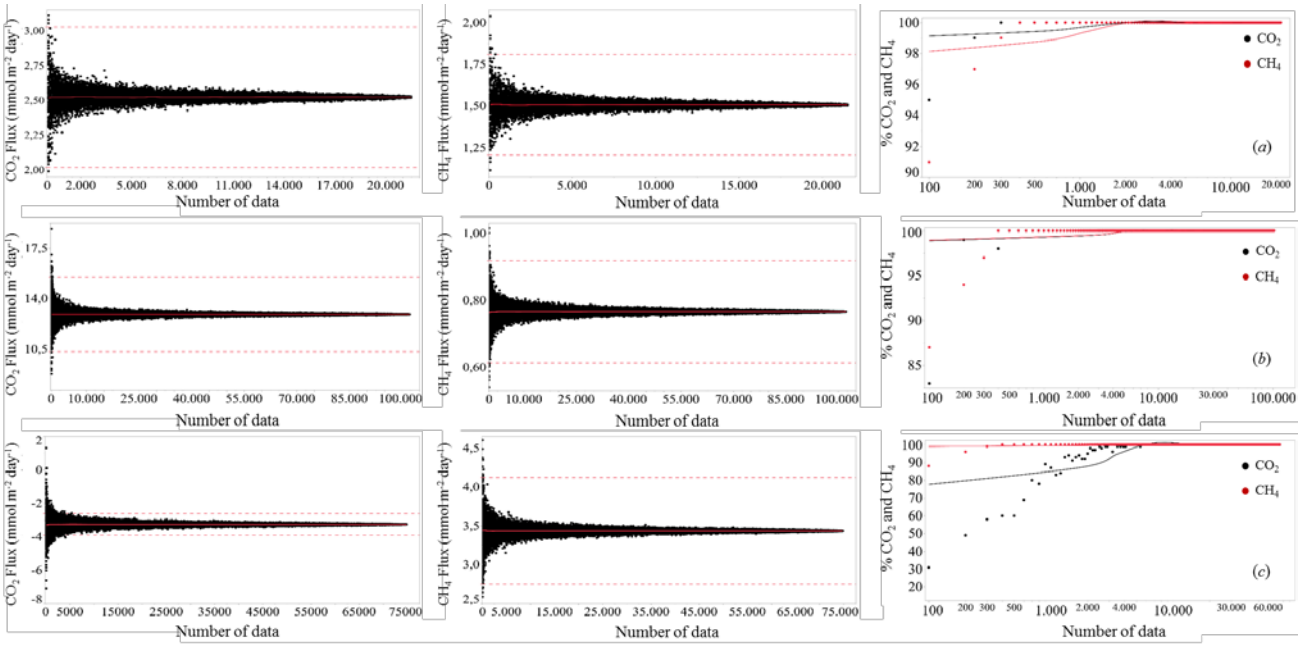

Figure 9: Analysis of number of diffusive fluxes required to capture the uncertainties in the CO_2 and CH_4 in: (a) CDU, (b) CUN and (c) FNS; within ± 20% of the mean flux (represented by the red dashed lines) from all diffusive fluxes measurements during the dry period. The solid line represents the average of diffusive fluxes of CO_2 and CH_4 in each scenario.

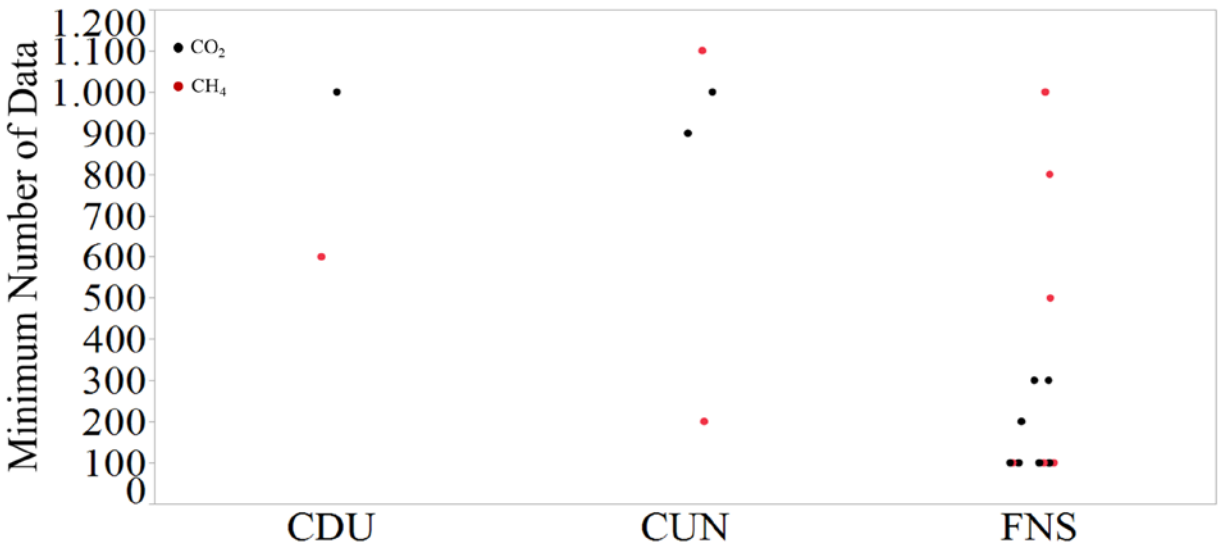

Figure 10: Distribution of minimum sampling effort values in CDU, CUN and FNS based in areas with the same size as CDU.

3.7 Bathymetry and its impact on diffusive fluxes of CO_2 and CH_4

The seismic profile in CDU showed a maximum depth of 25 m (average 10 m). In CUN, the maximum depth was 17 m (average 9 m) and in FNS the maximum depth was 64 m (average 15 m), during the dry period. The highest values of diffusive flux of CO_2 were observed in depths which ranging from 1 to 14 m in CDU. When related to CUN, the highest values were observed in 6 m depth, and in FNS were observed in 5 m depth. (Figure 11). On the other hand, when the diffusive flux of CH_4 was related to the bathymetry in CDU, the highest values were observed in 1 m depth. In CUN, the highest values were observed in 6 m depth, and in FNS were observed in 5 m depth. The spatial variability of diffusive flux of CO_2 and CH_4 were not statistically linked to depth in all reservoirs, except to CDU where a negative relationship between diffusive flux of CH_4 and depth was observed (Figure 11).

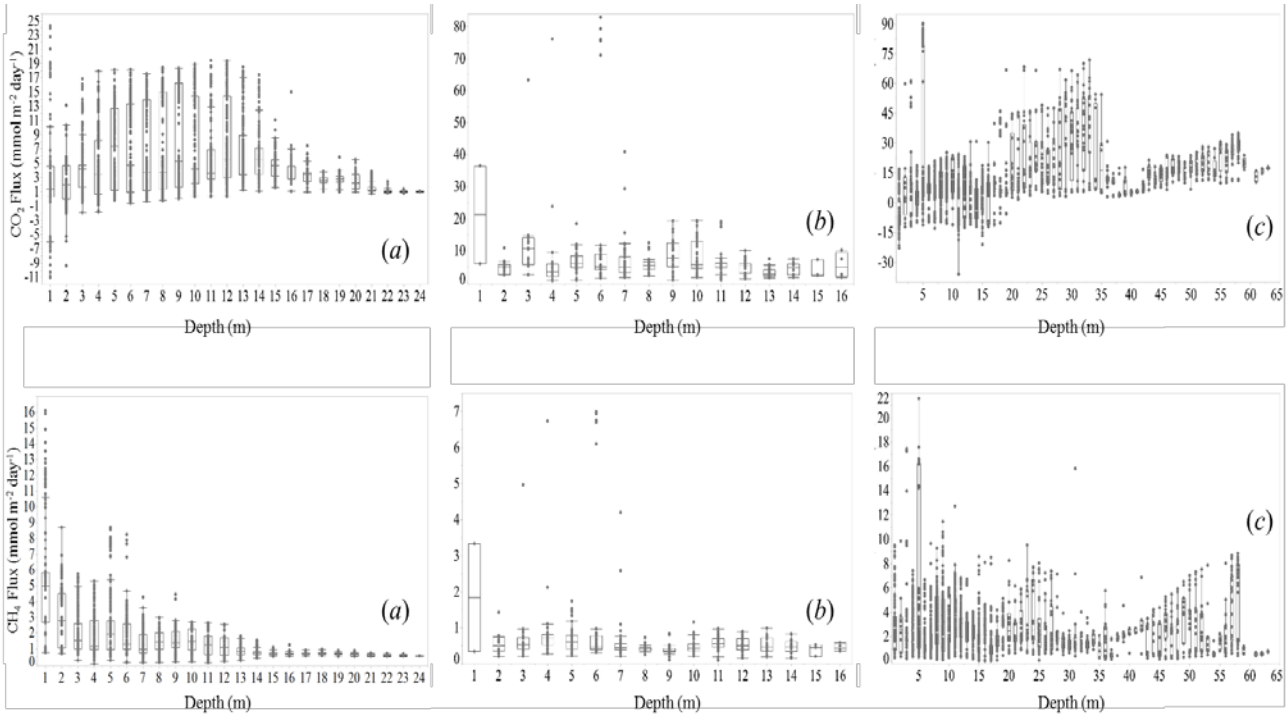

Figure 11: Distribution of diffusive fluxes of CO_2 and CH_4 (mmol m^{-2} day^{-1}) related to depth (m) in CDU (a), CUN (b) and FNS (c).

4. Discussion

This study shows large within-reservoir variability for CO_2 and CH_4 partial pressure and gas exchange velocity, which results in large spatial variability of CO_2 and CH_4 fluxes. According to the general assumption of a fixed *k* based on a single measured site at each dam, the diffusive fluxes of CO_2 and CH_4 were underestimated about ~38% and ~10%, respectively. When we use a fixed *k* based on average wind speed, the diffusive fluxes of CO_2 and CH_4 were underestimated about ~40% and ~80%, respectively. We also observed a persistently higher k_{600CH4} than k_{600CO2}.

4.1 Within-reservoir variability pCO_2 and pCH_4

The three reservoirs were predominantly supersaturated in CO_2 and CH_4 (Table 2) and therefore were sources of CO_2 and CH_4 to the atmosphere, even though influx of CO_2

was observed in some areas. The magnitude and variability of pCO_2 and pCH_4 reported here are in accordance with previous data reported for tropical and temperate reservoirs (Abril, Richard, and Guérin 2006; Roland et al. 2010; Teodoru, Prairie, and Del Giorgio 2011; Pacheco et al. 2015). We observed, for the first time, that riverine inflow areas are likely to have higher levels of pCO_2 and pCH_4 than the main river channel close to the dam. Conversely, pCH_4 was comparatively low close to the dam in all three reservoirs, while pCO_2 was comparatively low at the dam only in CDU; in CUN and FNS, pCO_2 close to the dam was relatively high, which in the case of CUN may be related to organic pollution by fish farms in the small bay south of the dam.

While our field measurements necessarily cover variability in space, but also in time, we ascribe the dam-inflow gradient of pCH_4 mainly to spatial variability. PLS regression models which included geographic location within a reservoir returned much higher degrees of explanation (r^2Y of 0.41-0.79) than corresponding models without geographic location (r^2Y of 0.12-0.55), and accordingly, geographic location was an important variable (VIP > 1; Table 3) in each PLS regression model explaining pCH_4. This implies that there are significant spatial gradients of pCH_4 along the main longitudinal axis of the reservoirs, as a result of the dam areas being cold spots of pCH_4 and river inflows being prone to be pCH_4 hot spots (Figure 6). CH_4 originates from OM degradation in sediments, and high sediment accumulation has been shown to result in a high OM supply to methanogenic microbes and therefore lead to high CH_4 production (Sobek et al. 2012). At river inflows, water slows down and sediment is deposited, often leading to the formation of Deltas at the inflow areas of reservoirs (Morris and Fan 1998). The frequently found high pCH_4 in river inflow areas (Figure 6) is therefore probably related to high sediment deposition in these areas (DelSontro et al. 2011; Maeck, Hofmann, and Lorke

2014). In addition, CH_4 imported from the catchment by inflowing rivers may contribute to the observed pattern (DelSontro et al. 2011; Mendonça et al. 2014).

Another reason for within-reservoir variability of pCO_2 and pCH_4 may be productivity. In general, pCO_2 correlated negatively with O_2 concentration and not strongly with geographic location (Table 3), indicating that reservoir-internal patterns in plankton productivity were important modulators of pCO_2. For example, a large part of the southern arm of FNS, where the eutrophic Sapucaí River (average TN: 1341.7 µg L^{-1}, average TP: 41.1 µg L^{-1}) enters the reservoir, pCO_2 was undersaturated (Figure 6). The CO_2 undersaturation in this eutrophic area can be explained by the intense CO_2 uptake during phytoplankton growth (chlorophyll *a* southern arm: 21.2 µg L^{-1} ± 14, northern arm: 9.8 µg L^{-1} ± 9 in the northern arm). An exception is CUN, where geographic location was an important predictor of pCO_2 (VIP > 1; Table 3), and the high pCO_2 in the river inflows may be attributed to either sediment OM degradation or riverine input of soil-derived CO_2. Interestingly, pCH_4 was high in this eutrophic southern arm of FNS, which could indicate that anaerobic decomposition of phytoplankton debris in the sediments results in CH_4 production. Accordingly, eutrophication has recently been pointed as a key driver of CH_4 fluxes in reservoirs at a global scale (Deemer et al. 2016). Similarly, also organic-rich effluent from local settlements may result in high pCH_4, such as close to the town ~12 km upstream the dam in CUN.

In addition, we cannot exclude that the variability of pCO_2 and pCH_4 is due to different types of flooded organic materials and the reservoir's morphometry (Roland et al. 2010; Teodoru, Prairie, and Del Giorgio 2011; Pacheco et al. 2015).

4.2 Within-reservoir variability in gas exchange velocity

We observed pronounced variability of the gas exchange coefficient k_{600} within all reservoirs. The registered values (average 0.9 ± 1.0 m day^{-1} from CO_2 and average 2.3 ± 2.4 m day^{-1} from CH_4) are in the range of reports by earlier studies (Vachon, Prairie, and Cole 2010; Prairie and del Giorgio 2013; McGinnis et al. 2015; Rantakari et al. 2015). There were positive but rather weak relationships between k_{600} and wind speed (Figure 7), and the PLS regression models were overall weak, indicating that k_{600} was not well predicable from the variables collected in this study. In some instances, we observed high k_{600} values in river inflow areas (Figure 6). In these areas, turbulence can be expected to be stronger than main reservoir body, which makes the water boundary layer unstable and enhances the gas exchange with the atmosphere. We also found higher k_{600} in some larger open areas (e.g. in the reservoir main stem of CUN). These areas are exposed to higher wind speed, which also increases the turbulence in the water surface (Figure 6). Since the gas exchange velocity is largely driven by water-side turbulence, it varies in space and time even at short scales, depending on water flow and the magnitude and direction of wind forcing. Evidently, this creates pronounced patterns in k_{600}, which are highly variable, not readily predictable, and not adequately represented by estimations of average k_{600} from wind speed.

4.3 Within-reservoir variability in diffusive CO_2 and CH_4 fluxes

As a result of the variabilities in concentrations and gas exchange velocities, diffusive flux of CO_2 varied between -36 and 90.2 mmol m^{-2} day^{-1} (6.1 ± 12.2, median: 4.5) and diffusive flux of CH_4 varied between 0.001 and 21.5 mmol m^{-2} day^{-1} (2 ± 2.2, median: 1.3) (Table 4). Diffusive CH_4 emission was higher in most river inflow areas compared to the respective dam basin (Figure 6). Also, several river inflow areas showed

high diffusive fluxes of CO_2, similar to the observations by Pacheco et al. 2015. Evidently, patterns of diffusive gas emission were entirely congruent with patterns in gas concentrations, because the gas exchange velocity was regulated by other factors than gas concentrations. It is important to consider that the observed within-reservoir patterns of diffusive CO_2 and CH_4 emission are snapshots in space and time: the k_{600} maps are the result of instantaneous and very local measurements, which are subject to rapid change depending on the water column and meteorological conditions, as well as the location of measurement. On the other hand, we consider the maps of gas concentration to reflect largely prevailing spatial patterns during the dry season. The fact that we could observe elevated CH_4 emission in most river inflow areas as compared to dam basins (Figure 6) is plausible because in inflow areas, high sediment deposition leads to high CH_4 production, and the relatively shallow water column minimizes the extent of CH_4 oxidation. In addition, water flow may be more turbulent in the proximity of the river, boosting the gas exchange velocity (Figure 6). While the mapping of surface water gas concentrations represents an important advance towards improved estimates of diffusive emission from reservoirs, it is clear that more research is needed on the variability and regulation of the gas exchange velocity in these large and morphologically complex systems. While the flux reported here was well covered in space, the year-around emission, which was not the point of the present paper, can also be highly heterogeneous. That said, it is important to point out that we do not recommend the assumption that the daily fluxes reported here can be used to calculate the yearly emission, especially to CUN where the sampling occurred in a such atypical moment for that reservoir (Figure 2).

Table 4: Average of k values (m day^{-1}) calculated by three different path (k_{FC}, k_d and k_{ws}) and their current fluxes of CO_2 and CH_4 (mmol m^{-2} day^{-1}) expressed by average ± standard deviation and range.

	CDU	CUN	FNS
$k_{FC\text{-}CO2}$ (m day^{-1})	2.2	0.7	1
$k_{FC\text{-}CH4}$ (m day^{-1})	4	1.9	4.5
$k_{d\text{-}CO2}$ (m day^{-1})	0.3	0.5	0.9
$k_{d\text{-}CH4}$ (m day^{-1})	2.4	1.5	3.3
$k_{ws\text{-}CO2}$ (m day^{-1})	0.8	1.2	0.6
$k_{ws\text{-}CH4}$ (m day^{-1})	0.8	1.2	0.6
CO_2 Flux using $k_{FC\text{-}CO2}$	4.8 ± 6 (-26.4 - 24.2)	7.7 ± 9.5 (0.6 - 83)	7.1 ± 15.8 (-36 - 90.2)
CH_4 Flux using $k_{FC\text{-}CH4}$	1.7 ± 1.7 (0.04 - 16)	0.6 ± 0.8 (0.1 - 7)	2.6 ± 2.5 (0.001 - 21.5)
CO_2 Flux using $k_{d\text{-}CO2}$	0.7 ± 0.7 (-0.9 - 4.7)	5.5 ± 3.3 (0.9 - 18.5)	6.3 ± 17.3 (-14.3 - 102)
CH_4 Flux using $k_{d\text{-}CH4}$	0.9 ± 0.7 (0.4 - 5.4)	0.5 ± 0.2 (0.1 - 1.5)	2.7 ± 3.4 (0.2 - 29)
CO_2 Flux using $k_{ws\text{-}CO2}$	2.1 ± 2.1 (-2.7 - 13.4)	13 ± 8 (2.2 - 44.3)	4.2 ± 11.6 (-9.7 - 69)
CH_4 Flux using $k_{ws\text{-}CH4}$	0.3 ± 0.2 (0.1 - 1.9)	0.4 ± 0.2 (0.08 - 1.2)	0.5 ± 0.6 (0.04 - 5.5)

4.4 Extrapolating the diffusive fluxes of CO_2 and CH_4 using single k values

The diffusive fluxes of CO_2 and CH_4 were measured through three different pathways, which differ in the way that we have calculated *k*. First, *k* for each gas was calculated based on FC measurements, deployed at several sites of each reservoir (k_{FC}). Second, we adapted a single *k* value, measured at the dam site at each reservoir (k_d). Third, we calculated *k* based on average wind speed from each reservoir (k_{ws}). Average, standard

deviation and range of *k* values and the diffusive fluxes of CO_2 and CH_4 calculated by these three different ways of calculation are exposed in Table 4.

Assuming that the real fluxes were measured using k_{FC} values, the real diffusive fluxes of CO_2 show higher spatial variability than other pathways among reservoirs (Figure 12), as is expected when we use several multiplier values. The same pattern was observed for diffusive fluxes of CH_4 from CDU and CUN, except for FNS where the use of $k_{d\text{-}CH4}$ shows higher variation in the calculations (Figure 12).

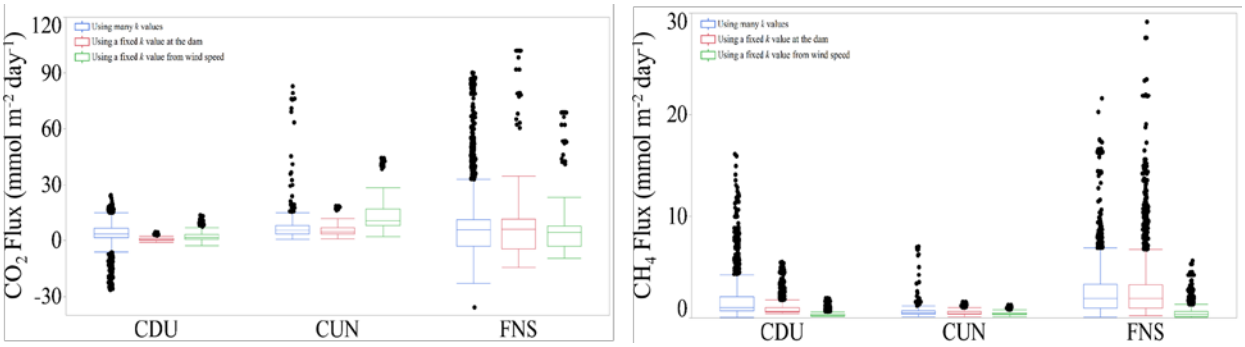

Figure 12: Box plot of CO_2 and CH_4 fluxes, measured by equilibrator using three different k calculated, from CDU, CUN and FNS reservoirs (mmol m^{-2} day^{-1}).

Taking into account the real flux premise, the diffusive flux of CO_2 using $k_{d\text{-}CO2}$ in CDU was underestimated about ~86% (0.7 mmol m^{-2} day^{-1}), ~26% in CUN (5.5 mmol m^{-2} day^{-1}) and ~11% (6.3 mmol m^{-2} day^{-1}) in FNS. For the diffusive flux of CH_4, the use of $k_{d\text{-}CH4}$ in CDU underestimated about ~44% (0.9 mmol m^{-2} day^{-1}) and ~17% in CUN (0.5 mmol m^{-2} day^{-1}). However, it overestimated about ~8% (2.7 mmol m^{-2} day^{-1}) of the real CH_4 fluxes in FNS.

When we fixed a single *k* value by taking one average wind speed for each reservoir, the diffusive flux of CO_2 was underestimated about ~57% (2.1 mmol m^{-2} day^{-1}) for CDU and ~41% (4.2 mmol m^{-2} day^{-1}) for FNS. For CUN in contrast, the use of $kws_{\text{-}CO2}$ overestimated the real flux about ~70% (13.1 mmol m^{-2} day^{-1}). For the diffusive flux of

CH_4, kws_{-CH4} underestimated the real fluxes about ~82% (0.3 mmol m^{-2} day^{-1}) in CDU, ~34% (0.4 mmol m^{-2} day^{-1}) in CUN and ~80% (0.5 mmol m^{-2} day^{-1}) in FNS. These fluctuations in the flux estimates are explained directly by the *k* values applied on the calculations.

4.5 Minimum sampling effort

We considered that our sampling strategies were representative in all reservoirs sampled according to our results about the minimum sampling efforts presented above. In CDU, the coefficients of variation (CV) for diffusive flux of CO_2 and CH_4 were 1.2 and 1, respectively. The similarity of their CV explains, in parts, the proximity of minimum numbers necessary to perform a representative sampling during the dry period. In CUN, the CV for CO_2 and CH_4 were equal (1.2), and we found that the minimum number of sampling points needed to perform a 90% reliability sampling in diffusive fluxes of CH_4 were similar. In FNS, the CV for CO_2 were two times higher than the CV of CH_4 (2.2 and 1, respectively), which explains the necessity of approximately five times more minimum sample points to cover the reservoir representatively (Figure 9).

Different regions of CUN and FNS required different minimum sampling effort to generate representative estimates of diffusive fluxes of CO_2 and CH_4 in an area corresponding in size to CDU (Figure 10). This means that sampling area is not a strong predictor for the minimum sampling effort, and local factors such as primary production, trophic state, depth, morphometry, flooded soil composition, river entrances, etc., may regulate the spatial variability of diffusive fluxes. Even though in larger reservoirs such as FNS, there are regions which are very homogeneous (i.e. have less spatial variability) and thus require lower sampling effort. However, there are also regions with high spatial variability (heterogeneous) that require higher sampling effort (Figure 10). We conclude

that also in larger reservoirs, sampling with high spatial resolution is needed to cover representatively the system.

The model previously presented by Wik et al. 2016 was adapted to CDU, CUN and FNS reservoirs. We emphasize that each aquatic system presents specific characteristics, which may perform different biogeochemical processes that directly or indirectly affect the estimate of minimum sampling effort.

4.6 Effect of water column depth on diffusive fluxes of CO_2 and CH_4 in CDU

Shallow water sediments are exposed to lower hydrostatic pressure than deep sediment, which allows the release of bubbles from the sediment into the water. Parts of these bubbles may dissolve in water and substantially increase the diffusive flux of CH_4. This is in agreement with studies that attributed high rates and frequency of CH_4 emissions to 1 to 7 m deep areas (Bastviken et al. 2004; DelSontro et al. 2011). Other studies found a negative relationship between water depth and CH_4 emission that was based on surface chambers and air pressure measurements (Figure 11) (Mattson and Likens 1990; Casper et al. 2000; Bastviken et al. 2004; DelSontro et al. 2011).

In CDU and CUN, we can see that after 6 m depth the diffusive flux of CH_4 decreases with increasing depth (Figure 11). In deep areas (> 15 m), we expect high sedimentation rates (Mendonça et al. 2014) but low values of CH_4 emission, due to hydrostatic pressure which can trap bubbles in the sediment. On the other hand, in FNS we can observe, in parts, the same pattern. However, after 40 m depth we observed that the diffusive flux of CH_4 increases with increasing the depth (Figure 11). Regions with 40 m of depth, or more, were detected in locations close to the dam in FNS, where hot spots of CH_4 emission were observed arising from small river inlets. Complementary, we did not observe any depth-flux dependence for diffusive CO_2 fluxes. As described above, diffusion

is the main pathway for CO_2 emission due to the high solubility of the gas in the water (1,7 g L^{-1}), which in parts can explain the homogeneous emission of CO_2 in different depths.

4.7 Persistence of higher k_{600CH4} values than k_{600CO2}

We found a persistence of $k_{600CH4} > k_{600CO2}$ for all reservoirs (Figure 7). Expressing a ratio k_{600CH4} / k_{600CO2}, the average of k_{600CH4} values were 2.8 times higher than the k_{600CO2} and there were no differences among reservoirs.

According to Fickian transport, k_{600CO2} values should be similar to k_{600CH4} values because the speed of diffusion for these gases is similar (Rantakari et al. 2015). However, such persistence in the k_{600CH4} values were consistently higher than k_{600CO2} values indicates that the two gases behave differently. The ratio k_{600CH4} / k_{600CO2} we found in this study is in agreement with observations by Prairie and del Giorgio 2013 and McGinnis et al. 2015, who suggest the presence of semistable CH_4 microbubbles to explain why k_{600CH4} is constantly higher than k_{600CO2}. It is important to note that the majority of our FC measurements have been done at the deepest points of each reservoir, over short time intervals (5 minutes) and covering a small surface area, which reduces the probability of capturing huge CH_4 bubbles as previously described by Prairie and del Giorgio 2013. Thus, most gas accumulation rates in the FC were linear over the 5 minute measurement intervals.

5. Implications

Many studies have suggested that FC is an efficient and cheap technique to predict k_{600} for different gases (Cole et al. 2010; Vachon, Prairie, and Cole 2010). The process behind the gas exchange in the air-water interface is complex however, which creates large uncertainties in the models to estimate *k*. More studies are needed to understand and explain how theses process acts naturally.

In summary, the high spatial variability in CO_2 and CH_4 concentrations, gas exchange velocities and fluxes, illustrated for the first time in the same study, are linked to different internal and external forces of each reservoir. Our results describe the influence of rivers of different characteristics on CO_2 and CH_4 emission, in which may also directly and indirectly influence the estimates for *k*. For out-scaling purposes, our spatial measurements in all reservoirs showed that estimates based on few points underestimate the real flux about 50%. In addition, the processes behind diffusive fluxes vary significantly for reservoirs of different trophic states, size, age and geographic positions. Although there are uncertainties in our estimates, we show that the diffusive fluxes of CO_2 and CH_4 are spatially scattered in these systems.

The scarcity of studies in tropical reservoirs, as well as the gaps in biogeochemical process included, create challenges to the understanding of carbon cycling in reservoirs, and hence, to achieve accurate estimates. Our findings provide valuable information on how to develop field-sampling strategies to perform representative fieldworks.

6. References

Abril, Gwenaël, Sandrine Richard, and Frédéric Guérin. 2006. 'In situ measurements of dissolved gases (CO 2 and CH 4) in a wide range of concentrations in a tropical reservoir using an equilibrator', *Science of the Total Environment*, 354: 246-51.

Algesten, G., S. Sobek, A. K. Bergstrom, A. Jonsson, L. J. Tranvik, and M. Jansson. 2005. 'Contribution of sediment respiration to summer CO2 emission from low productive boreal and subarctic lakes', *Microb Ecol*, 50: 529-35.

Almeida, Rafael M, Gabriel N Nóbrega, Pedro C Junger, Aline V Figueiredo, Anízio S Andrade, Caroline GB de Moura, Denise Tonetta, Ernandes S Oliveira Jr, Fabiana Araújo, and Felipe Rust. 2016. 'High Primary Production Contrasts with Intense Carbon Emission in a Eutrophic Tropical Reservoir', *Frontiers in microbiology*, 7.

Barros, Nathan, Jonathan J Cole, Lars J Tranvik, Yves T Prairie, David Bastviken, Vera LM Huszar, Paul Del Giorgio, and Fábio Roland. 2011. 'Carbon emission from hydroelectric reservoirs linked to reservoir age and latitude', *Nature Geoscience*, 4: 593-96.

Bastviken, David, Jonathan Cole, Michael Pace, and Lars Tranvik. 2004. 'Methane emissions from lakes: Dependence of lake characteristics, two regional assessments, and a global estimate', *Global biogeochemical cycles*, 18.

Bastviken, David, Lars J Tranvik, John A Downing, Patrick M Crill, and Alex Enrich-Prast. 2011. 'Freshwater methane emissions offset the continental carbon sink', *Science*, 331: 50-50.

Borges, Alberto V, François Darchambeau, Cristian R Teodoru, Trent R Marwick, Fredrick Tamooh, Naomi Geeraert, Fredrick O Omengo, Frédéric Guérin, Thibault

Lambert, and Cédric Morana. 2015. 'Globally significant greenhouse-gas emissions from African inland waters', *Nature Geoscience*, 8: 637-42.

Casper, Peter, Stephen C Maberly, Grahame H Hall, and Bland J Finlay. 2000. 'Fluxes of methane and carbon dioxide from a small productive lake to the atmosphere', *Biogeochemistry*, 49: 1-19.

Cole, Jonathan J, Darren L Bade, David Bastviken, Michael L Pace, and Matthew Van de Bogert. 2010. 'Multiple approaches to estimating air-water gas exchange in small lakes', *Limnology and Oceanography: Methods*, 8: 285-93.

Cole, Jonathan J, and Nina F Caraco. 1998. 'Atmospheric exchange of carbon dioxide in a low-wind oligotrophic lake measured by', *Limnology and Oceanography*, 43: 647-56.

Cole, Jonathan J, Nina F Caraco, George W Kling, and Timothy K Kratz. 1994. 'Carbon dioxide supersaturation in the surface waters of lakes', *Science-AAAS-Weekly Paper Edition*, 265: 1568-69.

Deemer, Bridget R, John A Harrison, Siyue Li, Jake J Beaulieu, Tonya DelSontro, Nathan Barros, José F Bezerra-Neto, Stephen M Powers, Marco A dos Santos, and J Arie Vonk. 2016. 'Greenhouse Gas Emissions from Reservoir Water Surfaces: A New Global Synthesis', *BioScience*: biw117.

Delmas, Robert, Corinne Galy -Lacaux, and greenhouse gases from the tropical hydroelectric reservoir of Petit Saut (French Guiana) compared with emissions from thermal alternatives', *Global Biogeochemical Cycles*, 15: 993-1003.

DelSontro, Tonya, Daniel F McGinnis, Sebastian Sobek, Ilia Ostrovsky, and Bernhard Wehrli. 2010. 'Extreme methane emissions from a Swiss hydropower reservoir: contribution from bubbling sediments', *Environmental science & technology*, 44: 2419-25.

Fearnside, Philip M, and Salvador Pueyo. 2012. 'Greenhouse-gas emissions from tropical dams', *Nature Climate Change*, 2: 382-84.

Galy-Lacaux, Cori

Labroue, Sandrine Richard, and Philippe Gosse. 1997. 'Gaseous emissions and oxygen consumption in hydroelectric dams: A case study in French Guyana', *Global Biogeochemical Cycles*, 11: 471-83.

Galy-Lacaux, Cori

Gosse. 1999. 'Long-term greenhouse gas emission

in tropical forest regions', *Global Biogeochemical Cycles*, 13: 503-17.

Gonzalez-Valencia, Rodrigo, Felipe Magana-Rodriguez, Oscar Gerardo-Nieto, Armando Sepulveda-Jauregui, Karla Martinez-Cruz, Katey Walter Anthony, Doug Baer, and Frederic Thalasso. 2014. 'In situ measurement of dissolved methane and carbon dioxide in freshwater ecosystems by off-axis integrated cavity output spectroscopy', *Environmental science & technology*, 48: 11421-28.

Guérin, Frédéric, Gwenaël Abril, Dominique Serça, Claire Delon, Sandrine Richard, Robert Delmas, Alain Tremblay, and Louis Varfalvy. 2007. 'Gas transfer velocities of CO 2 and CH 4 in a tropical reservoir and its river downstream', *Journal of Marine Systems*, 66: 161-72.

Höskuldsson, Agnar. 1988. 'PLS regression methods', *Journal of chemometrics*, 2: 211-28.

Hu, Yuanan, and Hefa Cheng. 2013. 'The urgency of assessing the greenhouse gas budgets of hydroelectric reservoirs in China', *Nature Climate Change*, 3: 708-12.

IBGE, Diretoria de Pesquisas. 2012. 'Coordenação de Agropecuária', *Produção Pecuária Municipal*: 1-55.

Jähne, Bernd, Karl Otto Münnich, Rainer Bösinger, Alfred Dutzi, Werner Huber, and Peter Libner. 1987. 'On the parameters influencing air water gas exchange', *Journal of Geophysical Research: Oceans*, 92: 1937-49.

Kemenes, Alexandre, Bruce Rider Forsberg, and John Michael Melack. 2007. 'Methane release below a tropical hydroelectric dam', *Geophysical research letters*, 34.

Louis, Vincent L St, Carol A Kelly, Éric Duchemin, John WM Rudd, and David M Rosenberg. 2000. 'Reservoir Surfaces as Sources of Greenhouse Gases to the Atmosphere: A Global Estimate Reservoirs are sources of greenhouse gases to the atmosphere, and their surface areas have increased to the point where they should be included in global inventories of anthropogenic emissions of greenhouse gases', *BioScience*, 50: 766-75.

Maeck, Andreas, Hilmar Hofmann, and Andreas Lorke. 2014. 'Pumping methane out of aquatic sediments: ebullition forcing mechanisms in an impounded river', *Biogeosciences*, 11: 2925-38.

Mattson, Mark D, and Gene E Likens. 1990. 'Air pressure and methane fluxes'.

McGinnis, Daniel F, Georgiy Kirillin, Kam W Tang, Sabine Flury, Pascal Bodmer, Christof Engelhardt, Peter Casper, and Hans-Peter Grossart. 2015. 'Enhancing surface methane fluxes from an oligotrophic lake: exploring the microbubble hypothesis', *Environmental science & technology*, 49: 873-80.

Mendonça, Raquel, Sarian Kosten, Sebastian Sobek, Jonathan J Cole, Alex C Bastos, Ana Luiza Albuquerque, Simone J Cardoso, and Fábio Roland. 2014. 'Carbon sequestration in a large hydroelectric reservoir: an integrative seismic approach', *Ecosystems*, 17: 430-41.

MME, EPE. 2013. 'Plano Decenal de Expansão de Energia 2022', *Brasılia: Ministério de Minas e Energia—MME. Empresa de Pesquisa Energética—EPE*.

Morris, Gregory L, and Jiahua Fan. 1998. *Reservoir sedimentation handbook: design and management of dams, reservoirs, and watersheds for sustainable use* (McGraw Hill Professional).

Myhre, Gunnar, Drew Shindell, François-Marie Bréon, William Collins, Jan Fuglestvedt, Jianping Huang, Dorothy Koch, Jean-François Lamarque, David Lee, and Blanca Mendoza. 2013. 'Anthropogenic and natural radiative forcing', *Climate change*, 423.

Pacheco, FS, MCS Soares, AT Assireu, MP Curtarelli, F Roland, G Abril, JL Stech, PC Alvalá, and JP Ometto. 2015. 'The effects of river inflow and retention time on the spatial heterogeneity of chlorophyll and water–air CO 2 fluxes in a tropical hydropower reservoir', *Biogeosciences*, 12: 147-62.

Prairie, Yves, and Paul del Giorgio. 2013. 'A new pathway of freshwater methane emissions and the putative importance of microbubbles', *Inland Waters*, 3: 311-20.

Rantakari, Miitta, Jouni Heiskanen, Ivan Mammarella, Tiina Tulonen, Jessica Linnaluoma, Paula Kankaala, and Anne Ojala. 2015. 'Different apparent gas exchange coefficients for CO2 and CH4: Comparing a brown-water and a clear-water lake in the boreal zone during the whole growing season', *Environmental science & technology*, 49: 11388-94.

Raymond, Peter A, Jens Hartmann, Ronny Lauerwald, Sebastian Sobek, Cory McDonald, Mark Hoover, David Butman, Robert Striegl, Emilio Mayorga, and Christoph Humborg. 2013. 'Global carbon dioxide emissions from inland waters', *Nature*, 503: 355-59.

Roland, Fábio, Luciana O Vidal, Felipe S Pacheco, Nathan O Barros, Arcilan Assireu, Jean PHB Ometto, André CP Cimbleris, and Jonathan J Cole. 2010. 'Variability of carbon dioxide flux from tropical (Cerrado) hydroelectric reservoirs', *Aquatic Sciences*, 72: 283-93.

Smith, SV. 1985. 'Physical, chemical and biological characteristics of CO2 gas flux across the air *Water, Air, & Soil Pollution*, 8: 387-98.

Sobek, Sebastian, Tonya DelSontro, Nuttakan Wongfun, and Bernhard Wehrli. 2012. 'Extreme organic carbon burial fuels intense methane bubbling in a temperate reservoir', *Geophysical research letters*, 39.

Sobek, Sebastian, Lars J Tranvik, and Jonathan J Cole. 2005. 'Temperature independence of carbon dioxide supersaturation in global lakes', *Global Biogeochemical Cycles*, 19.

Teodoru, Cristian R, Yves T Prairie, and Paul A Del Giorgio. 2011. 'Spatial heterogeneity of surface CO2 fluxes in a newly created Eastmain-1 reservoir in northern Quebec, Canada', *Ecosystems*, 14: 28-46.

Vachon, Dominic, Yves T Prairie, and Jonathan J Cole. 2010. 'The relationship between near-surface turbulence and gas transfer velocity in freshwater systems and its implications for floating chamber measurements of gas exchange', *Limnology and Oceanography*, 55: 1723.

Wanninkhof, Rik. 1992. 'Relationship between wind speed and gas exchange over the ocean', *Journal of Geophysical Research: Oceans*, 97: 7373-82.

Weiss, R_F. 1974. 'Carbon dioxide in water and seawater: the solubility of a non-ideal gas', *Marine chemistry*, 2: 203-15.

Wik, Martin, Brett F Thornton, David Bastviken, Jo Uhlbäck, and Patrick M Crill. 2016. 'Biased sampling of methane release from northern lakes: A problem for extrapolation', *Geophysical research letters*.

Xiong, Wei, Ian Holman, Erda Lin, Declan Conway, Yue Li, and Wenbin Wu. 2012. 'Untangling relative contributions of recent climate and CO2 trends to national cereal production in China', *Environmental Research Letters*, 7: 044014.

Yamamoto, Sachio, James B Alcauskas, and Thomas E Crozier. 1976. 'Solubility of methane in distilled water and seawater', *Journal of Chemical and Engineering Data*, 21: 78-80.